

Search for the dark photon in the π^0 decay

R. Fantechi^{*†}

INFN - Sezione di Pisa and CERN

E-mail: fantechi@cern.ch

The NA48/2 Collaboration has analyzed a sample of $1.7 \cdot 10^7$ $\pi^0 \rightarrow \gamma e^+ e^-$ collected at CERN in 2003-2004 to search for dark photon (A') production and decay in the chain $\pi^0 \rightarrow \gamma A', A' \rightarrow e^+ e^-$. No signal has been observed and an exclusion region in the plane of A' mass and mixing parameter has been established, more stringent than the previous one in the A' mass range between 9 and 70 MeV/c^2

The European Physical Society Conference on High Energy Physics

22–29 July 2015

Vienna, Austria

^{*}Speaker.

[†]for the NA48/2 Collaboration: Cambridge, CERN, Chicago, Dubna, Edinburgh, Ferrara, Firenze, Mainz, North-western, Perugia, Pisa, Saclay, Siegen, Torino, Wien.

1. Introduction

The NA48/2 experiment at CERN has collected a large sample of kaon decays in flight, of the order of about $2 \cdot 10^{11}$ decays in the fiducial volume. These decays are also a source of tagged π^0 decays, useful for precision measurements. One example is the search for a hypothetical dark photon (DP, denoted A').

In a rather general set of hidden sector models with an extra U(1) gauge symmetry [1], the interaction of the DP with the visible sector proceeds through kinetic mixing with the Standard Model (SM) hypercharge. Such scenarios with GeV-scale dark matter provide possible explanations to the observed rise in the cosmic-ray positron fraction with energy and the muon gyromagnetic ratio ($g - 2$) measurement [2]. Characterization of the DP passes through two a priori unknown parameters, the mass $m_{A'}$ and the mixing parameter ε^2 . Production in the π^0 decay and the subsequent decay proceed via the chain $\pi^0 \rightarrow \gamma A', A' \rightarrow e^+ e^-$. The expected branching fraction of the above π^0 decay is [3]

$$\mathcal{B}(\pi^0 \rightarrow \gamma A') = 2\varepsilon^2 \left(1 - \frac{m_{A'}^2}{m_{\pi^0}^2}\right)^3 \mathcal{B}(\pi^0 \rightarrow \gamma\gamma)$$

with a kinematical suppression for $m_{A'}$ near the mass of the π^0 . For A' masses below the π^0 mass, the only allowed tree-level decay into SM fermions is $A' \rightarrow e^+ e^-$. The expected total decay width is

$$\Gamma_{A'} \approx \Gamma(A' \rightarrow e^+ e^-) = \frac{1}{3} \alpha \varepsilon^2 m_{A'} \sqrt{1 - \frac{4m_e^2}{m_{A'}^2}} \left(1 + \frac{2m_e^2}{m_{A'}^2}\right)$$

For $2m_e < m_{A'} < m_{\pi^0}$, the DP mean proper lifetime is

$$c\tau_{A'} = \hbar c / \Gamma_{A'} \approx 0.8 \mu\text{m} \cdot \left(\frac{10^{-6}}{\varepsilon^2}\right) \cdot \left(\frac{100\text{MeV}/c^2}{m_{A'}}\right)$$

These proper lifetime translates in a maximum mean path in the NA48/2 reference system, for a maximum energy of 50 GeV, of

$$L_{max} \approx (E_{max}/m_{A'}) c\tau \approx 0.4\text{mm} \cdot \left(\frac{10^{-6}}{\varepsilon^2}\right) \cdot \left(\frac{100\text{MeV}}{m_{A'}}\right)^2$$

This analysis is performed assuming that the DP decays at the production point (prompt decay), which is valid for sufficiently large values of $m_{A'}$ and ε^2 . In this case, the DP production and decay signature is identical to that of the Dalitz decay $\pi_D^0 \rightarrow e^+ e^- \gamma$ which therefore represents an irreducible, but well controlled background and determines the sensitivity. The NA48/2 experiment provides pure π_D^0 decay samples through the reconstruction of $K^\pm \rightarrow \pi^\pm \pi^0$ and $K^\pm \rightarrow \pi^0 \mu^\pm \nu$, in the following $K_{2\pi}$ and $K_{\mu 3}$.

2. The NA48/2 beam

The beam line used in the NA48/2 [4] data taking was specifically designed to simultaneously transport positive and negative particles. The two simultaneous K^+ and K^- beams were produced by 400 GeV primary protons from the CERN SPS impinging on a 40 cm long beryllium target.

Opposite charge particles, with a central momentum of 60 GeV/c and a momentum band of $\pm 3.8\%$ (rms), were selected by two systems of dipole magnets (each forming an “achromat”), focusing quadrupoles, muon sweepers and collimators. At the entrance of the decay volume, a 114 m long evacuated vacuum tank, the beams contained $\sim 2.3 \cdot 10^6 K^+$ and $\sim 1.3 \cdot 10^6 K^-$ per pulse of about 4.5 s duration with a flux ratio K^+/K^- close to 1.8. The two beams were focused ~ 200 m downstream of the production target in front of the first spectrometer chamber.

3. The NA48/2 detector

The momenta of charged decay products were measured by a magnetic spectrometer, housed in a tank filled with helium at nearly atmospheric pressure and placed after the decay volume. The spectrometer accommodated four drift chambers composed each of 8 planes of sense wires, and a dipole magnet located between the second and the third DCHs, which gave a horizontal transverse momentum kick to charged particles of 120 MeV/c. The corresponding measured spectrometer momentum resolution was $\sigma_p/p = 1.02\% \oplus 0.044\% p$, where the momentum p is expressed in GeV/c. A counter hodoscope consisting of two planes of orthogonal plastic scintillator strips producing fast trigger signals was placed after the spectrometer. A 127 cm ($27X_0$) thick liquid krypton electromagnetic calorimeter located further downstream is used to measure energy and position of photons and electrons. Its 13248 readout cells had a transverse size of 2×2 cm² each without longitudinal segmentation. The energy resolution was $\sigma_E/E = 3.2\%/\sqrt{E} \oplus 9\%/E \oplus 0.42\%$ (E in GeV). The spatial resolution for the transverse coordinates x and y of an isolated electromagnetic shower was $\sigma_x = \sigma_y = 0.42/\sqrt{E} \oplus 0.06$ cm (E in GeV). A dedicated two-level trigger has been used to collect three-track events with high efficiency. A description of the detector can be found in [5].

A Monte Carlo simulation based on GEANT3 [6] and including beamline and detector geometries, magnetic fields, local inefficiencies and misalignments, along with their possible time variations has been used to evaluate the detector response.

4. Event selection

To select $K_{2\pi}$ and $K_{\mu 3}$ decays followed by the prompt π^0 decay chain, a series of criteria were chosen, identical for the two decays, up to momentum, invariant mass and particle identification conditions. The main selection criteria are:

- Track segments from the upstream part of the spectrometer are extrapolated back, taking into account stray magnetic fields, Earth’s magnetic field and multiple scattering, to reconstruct three-track vertices.
- A three-track vertex formed by a pion or muon candidate and two electrons of opposite sign is required. Particle identification is based on the ratio E/p between the energy E in the LKr calorimeter and the momentum p in the spectrometer. Pion (muon) candidates are selected requiring $p > 5$ GeV/c and $E/p < 0.85$ ($E/p < 0.4$), respectively. Electrons should have $p > 2.75$ GeV/c and $0.85 < E/p < 1.15$ (the lower value being 0.80 if $p < 5$ GeV/c).

- The tracks from the vertex should be in the acceptance of the drift chambers, the LKr calorimeter and charged hodoscope. Their geometrical separation in the drift chamber and calorimeter planes should be larger than some minimum value to reject photon conversions and to minimize shower overlaps.
- A photon candidate is a single isolated LKr cluster, in time with the tracks, separated by the pion or muon candidate by at least 10 cm (25 cm) from the electron (pion, muon) candidate impact points and with energy larger than 3 GeV.
- The total reconstructed momentum of the three tracks should be between 53 and 67 GeV/c.
- An event is classified as $K_{2\pi}$ if the squared total transverse momentum with respect to the nominal axis (p_T^2) is below $5 \cdot 10^{-4} (\text{GeV}/c)^2$, while it is taken as a muon if $5 \cdot 10^{-4} < p_T^2 < 0.04 (\text{GeV}/c)^2$.
- The reconstructed invariant mass of the $e^+e^-\gamma$ system should be compatible with the π^0 mass within $\pm 8 \text{ MeV}/c^2$, 5 times the $m_{ee\gamma}$ resolution.
- For the $K_{2\pi}$ selection the invariant mass of the $\pi^\pm e^+ e^-\gamma$ system should be compatible with the K^\pm mass within $20 \text{ MeV}/c^2$.
- For the $K_{\mu 3}$ selection, the invariant mass $m_{miss}^2 = (P_K - P_\mu - P_{\pi^0})^2$ should be compatible with zero within $0.01 \text{ GeV}^2/c^4$.

The total number of kaon decays in the fiducial region is computed as

$$N_K = \frac{N_{2\pi D}}{[\mathcal{B}(K_{2\pi}A_\pi(K_{2\pi D}) + \mathcal{B}(K_{\mu 3}A_\pi(K_{\mu 3D}))]\mathcal{B}(\pi_D^0)e_1e_2}$$

where $N_{2\pi D}$ is the number of reconstructed candidates, A_π the acceptances for the $K_{2\pi^0}$ and $K_{\mu 3}$ decays obtained from the simulation, B are the branching ratios for the various modes and e_1, e_2 are the trigger efficiencies for L1 and L2 trigger algorithms, computed from downscaled control samples. The total number of kaon decays amounts to $(1.57 \pm 0.05) \cdot 10^{11}$, while the number of π^0 decays collected in the $K_{2\pi D}$ and $K_{\mu 3D}$ selections are $1.38 \cdot 10^7$ and $0.31 \cdot 10^7$, respectively, adding up to $1.69 \cdot 10^7$. In Figure 1 and 2 the reconstructed mass spectra ($m_{\pi ee\gamma}$, m_{miss}^2 , m_{ee}) are shown for data and normalized MC sample.

5. Simulation of the π_D^0 background

To evaluate the kaon flux and to estimate the irreducible π_D^0 background, simulations of $K_{2\pi}, K_{\mu 3}, K_{3\pi}$ with the π_D^0 decay are performed. For the first two decays, final-state radiation is included [7]. The π_D^0 decay is simulated using the lowest order differential rate [8]

$$\frac{d^2\Gamma}{dxdy} = \Gamma_0 \frac{\alpha}{\pi} |F(x)|^2 \frac{(1-x)^3}{4x} \left(1 + y^2 + \frac{r^2}{x}\right)$$

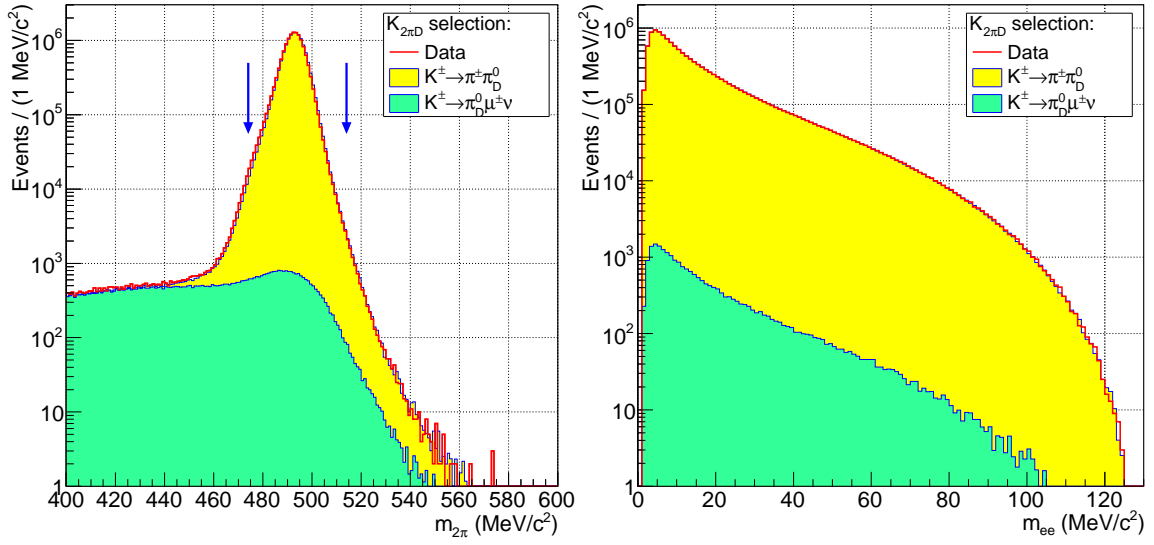


Figure 1: Invariant mass distributions of data and MC events for the $K_{2\pi D}$ selection. The signal region is indicated by the two arrows.

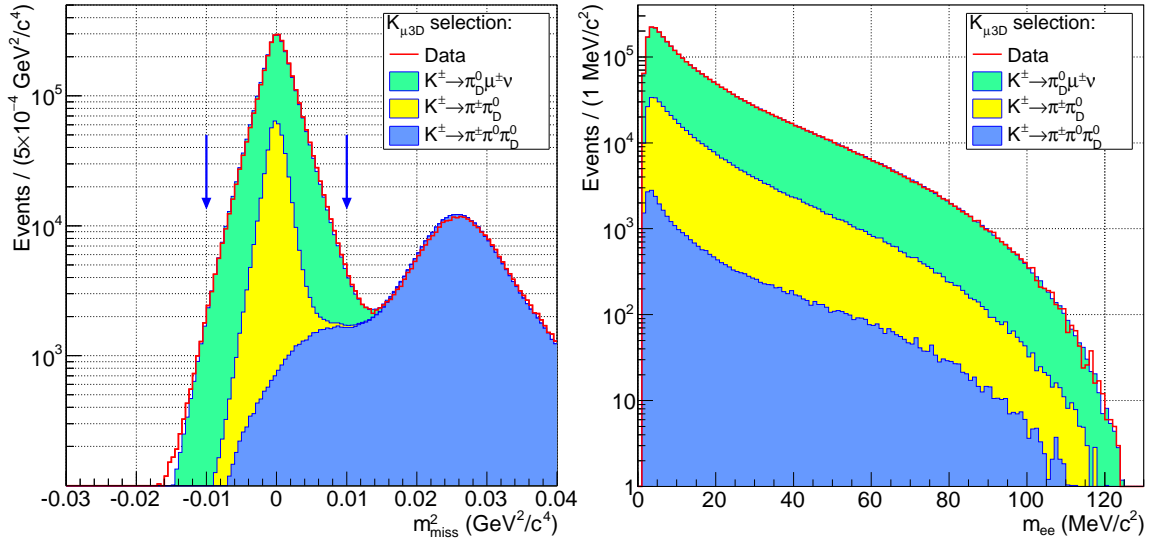


Figure 2: Invariant mass distributions of data and MC events for the $K_{\mu 3D}$ selection. The signal region is indicated by the two arrows.

where Γ_0 is the rate of the decay $\pi^0 \rightarrow \gamma\gamma$, $r = 2m_e/m_{\pi^0}$ and $F(x)$ is the pion transition form factor. The kinematical variables are

$$x = \frac{(Q_1 + Q_2)^2}{m_{\pi^0}^2} = (m_{ee}/m_{\pi^0})^2, \quad y = \frac{2P(Q_1 - Q_2)}{m_{\pi^0}^2(1-x)}$$

where Q_1, Q_2 and P are the four-momenta of the two electrons and the pion and m_{ee} is the invariant mass of the e^+e^- pair.

Radiative corrections to the π_D^0 decay are implemented following the approach of [8], revised to improve numerical precision [9]: the differential decay rate is modified by a factor function of x and y . Here inner bremsstrahlung photon emission is not simulated and its effects on the acceptance are not taken into account.

The pion transition form factor is not measured in this analysis, but an effective fit to the measured m_{ee} spectrum ensures a satisfactory background description in the kinematical range $m_{ee} > 8\text{MeV}/c^2$, as quantified by a χ^2 test. The region below this value is not considered due to the significantly larger uncertainties on the acceptance.

6. Search for the dark photon signal

The search for the dark photon is performed scanning different mass hypotheses with variable mass steps. The resolution on m_{ee} is evaluated with MC simulations and parametrized as $\sigma_m = 0.067 \text{ MeV}/c^2 + 0.0105 \cdot m_{ee}$. It determines the value of the mass step and the size of the DP mass window in the scan. The mass step is set to be $\sigma_m/2$ and the signal region for each DP window as $\pm 1.5\sigma_m$.

A total of 404 mass hypotheses in the range $9 \text{ MeV}/c^2 \leq m_{ee} \leq 120 \text{ MeV}/c^2$ have been tested. The lower limit on m_{ee} is due to the limited precision of the background simulation and the upper limit is determined by the drop to zero of the signal acceptance. Figure 3 displays the distribution of observed events (N_{obs}) in the signal region and the number of π_D^0 background events (N_{exp}) expected from the simulation, corrected by the trigger efficiencies.

The statistical significance of the dark photon signal is defined as

$$S = (N_{obs} - N_{exp}) / \sqrt{(\delta N_{obs})^2 + (\delta N_{exp})^2}$$

where $\delta N_{obs} = \sqrt{N_{obs}}$ is the statistical uncertainty on the number of observed events, and δN_{exp} is the larger uncertainty on the number of expected background events, coming mainly from the statistical error on the measured trigger efficiencies. The statistical significance of the dark photon signal is shown in Figure 3 as a function of the mass hypothesis, which nowhere exceeds 3.5, indicating that no significant DP signal is observed.

For each mass hypothesis, confidence intervals at 90% CL for the number of DP decay candidates (N_{DP}) are computed using the Rolke-Lopez method [10] from N_{obs} , N_{exp} , δN_{exp} , with the assumption of Poissonian errors on the number of events.

For each DP mass value, assuming it decays only in e^+e^- (good approximation for $m_{A'} < 2m_\mu$), upper limits on the branching fraction $\mathcal{B}(\pi^0 \rightarrow \gamma A')$ are computed using the relation

$$\mathcal{B}(\pi^0 \rightarrow \gamma A') = \frac{N_{DP}}{N_K e_1 e_2 [\mathcal{B}(K_{2\pi}) A_{DP}(K_{2\pi}) + \mathcal{B}(K_{\mu 3}) A_{DP}(K_{\mu 3}) + 2\mathcal{B}(K_{3\pi}) A_{DP}(K_{3\pi})]}$$

where A_{DP} are the acceptances for the various decay modes (followed by the prompt π^0 to DP decay chain) and e_1, e_2 the trigger efficiencies.

Acceptances for each DP mass value are computed from the simulation without radiative corrections to the π_D^0 decays, as such corrections are irrelevant in the π^0 to DP decay chain.

Upper limits on the mixing parameter ε^2 are obtained for each DP mass value using the above $\mathcal{B}(\pi^0 \rightarrow \gamma A')$ upper limits [11]. They are shown in Figure 4 together with limits from previous

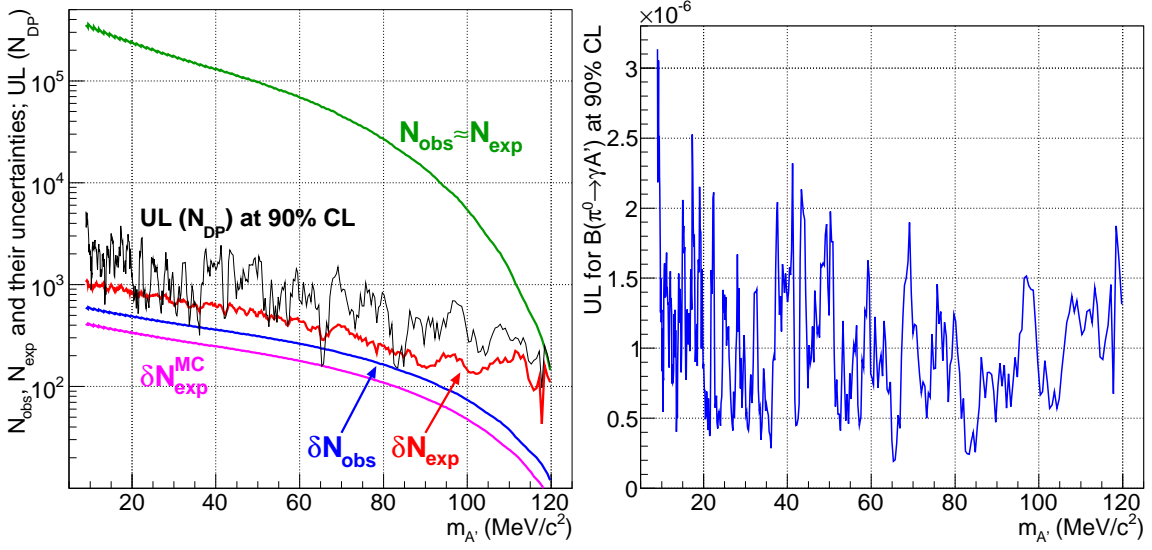


Figure 3: Left: Numbers of observed data (N_{obs}) and expected π_D^0 background events (N_{exp}), their estimated uncertainties and obtained limits on the number of DP events. Right: obtained upper limits at 90% CL on $B(\pi^0 \rightarrow \gamma A')$ as a function of the mass value.

experiments [12][13][14][15][16][17][18]. The plot shows also the band in the $(m_{A'}, \varepsilon^2)$ plane where the discrepancy between the measured and calculated muon $(g-2)$ values stays within two standard deviations because of the DP contribution. The region excluded by the electron $(g-2)$ measurement [2][19][20] is displayed as well. The best limit on ε^2 is obtained at low DP masses, where the kinematic suppression is small.

The assumption that the DP decays promptly can be verified a posteriori, translating the lowest limit obtained $\varepsilon^2 m_{A'}^2 = 3 \cdot 10^{-5} \text{MeV}^2/c^4$ into a maximum mean DP path of ≈ 10 cm, using the relation

$$L_{max} \approx \frac{E_{max}}{m_{A'} c^2} \cdot c \tau_{A'} \approx 0.4 \text{mm} \cdot \left(\frac{10^{-6}}{\varepsilon^2} \right) \cdot \left(\frac{100 \text{MeV}/c^2}{m_{A'}} \right)^2$$

to be compared with the resolution of the longitudinal coordinate of the three-track vertex, which is about 1 m.

7. Conclusions

Using data collected in 2003-2004, NA48/2 has performed a search for the dark photon (DP) production in the $\pi^0 \rightarrow \gamma A'$ decay followed by the prompt decay $A' \rightarrow e^+ e^-$. No dark photon signal has been observed, providing a more stringent upper limit for the ε^2 mixing parameter in the A' mass range 9-70 MeV/c^2 . The result rules out, in combination with other experimental searches, the DP as an explanation for the muon $(g-2)$ measurement, assuming that the DP couples to quarks and decays mainly to SM fermions.

References

- [1] B. Holdom, Phys. Lett. **B166** (1986) 196.

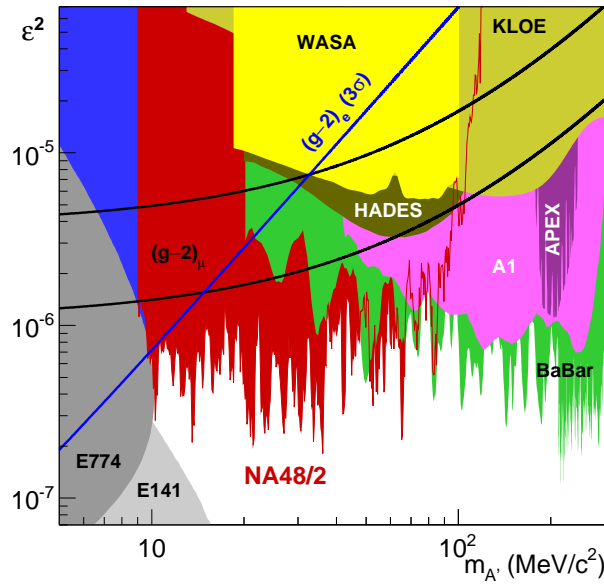


Figure 4: Upper limits at 90% CL on the mixing parameter ϵ^2 as a function of the DP mass $m_{A'}$, together with results from other experiments

- [2] M. Pospelov, Phys. Rev. **D80** (2009) 095002.
- [3] B. Batell, M. Pospelov and A. Ritz, Phys. Rev. **D80** (2009) 095024.
- [4] J. R. Batley *et al.*, Eur. Phys. J. **C52** (2007) 875.
- [5] V. Fanti *et al.*, NIM **A574** (2007) 433.
- [6] GEANT Detector Description and Simulation Tool, CERN Program Library W5013, 1994.
- [7] C. Gatti, Eur. Phys. J. **C45** (2006) 417.
- [8] K. O. Mikaelian and J. Smith, Phys. Rev. **D5** (1972) 1763.
- [9] T. Husek, K. Kampf and J. Novotny, arXiv:1504.06178.
- [10] W.A. Rolke and A.M.Lopez, Nucl. Instrm. Meth. **A458** (2001) 745.
- [11] J. R. Batley *et al.*, Phys. Lett. **B746** (2015) 178.
- [12] S. Andreas, C. Niebuhr and A. Ringwald, Phys. Rev. **D86** (2012) 095019.
- [13] D. Babusci *et al.* (KLOE-2 Collaboration), Phys. Lett. **B720** (2013) 111.
- [14] P. Adlarson *et al.* (WASA-at-COSY Collaboration), Phys. Lett. **B726** (2013) 187.
- [15] G. Agakishiev *et al.* (HADES Collaboration), Phys. Lett. **B731** (2014) 265.
- [16] H. Merkel *et al.* (A1 Collaboration), Phys. Rev. Lett. **112** (2014) 221802.
- [17] S. Abrahamyan *et al.* (APEX Collaboration), Phys. Rev. Lett. **107** (2011) 191804.
- [18] J.P. Lees *et al.* (BaBar Collaboration), Phys. Rev. Lett. **113** (2014) 201801.
- [19] M. Endo, K. Hamaguchi and G. Mishima, Phys. Rev. **D86** (2012) 095029.
- [20] H. Davoudiasl, H-S. Lee and W.J. Marciano, Phys. Rev. **D89** (2014) 095006.